

Intranuclear cascade calculation of high energy heavy ion collisions: Effect of interactions between cascade particles

Y. Yariv and Z. Fraenkel

Department of Nuclear Physics, Weizmann Institute of Science, Rehovot, Israel

(Received 15 October 1980)

Interactions between cascade particles were included in our intranuclear cascade calculation for high energy heavy ion collisions. This leads to better agreement between the calculated and experimental results for the inclusive pion cross sections and for two-nucleon correlations, without changing appreciably the calculated inclusive proton cross sections. The "single knockout" nucleons are shown to be a small fraction of the inclusive spectra.

NUCLEAR REACTIONS Calculated effect of interactions between cascade particles in the intranuclear cascade model of high-energy heavy-ion reactions. Inclusive proton and pion cross sections and two-particle correlations. $E = 400-1050$ MeV/nucleon. $^{12}\text{C} + ^{12}\text{C}$, $^{40}\text{Ar} + ^{40}\text{Ca}$, $^{40}\text{Ar} + ^{40}\text{Ar}$, $^{20}\text{Ne} + ^{238}\text{U}$, $^{40}\text{Ar} + ^{208}\text{Pb}$.

I. INTRODUCTION

In a recent paper¹ the intranuclear cascade (INC) model of high-energy hadron-nucleus reactions was applied to relativistic heavy-ion reactions. The approach was a direct generalization of the VEGAS calculation.² The calculation strives to treat fairly accurately the multiple collision processes in nuclei, but disregards completely the nucleon-nucleon correlations. It is based on concepts of relativistic classical mechanics, i.e., the momenta and coordinates (trajectories) of particles are treated classically. Both target and projectile are assumed initially to be cold Fermi gases in their respective potential wells. The nucleon-nucleon cross sections in the calculation are "on the mass shell," free nucleon-nucleon cross sections. The only quantum mechanical concept incorporated is the Pauli principle. The pions are produced and absorbed via Δ_{33} formation, decay, and capture.

The simulation process uses a "timelike basis" Monte Carlo procedure.² This procedure follows the states of all the cascade particles as a function of time. One advantage of using the timelike basis is the possibility of changing the global properties of the system as the interaction proceeds. Thus, the density of the relevant Fermi seas is depleted after each interaction.¹ Another advantage is the possibility of including interactions between the cascade particles, i.e., between any two particles both of which have already undergone one or more interactions during the cascade. Previous calculations^{1,2} neglected such interactions and included only collisions between particles of which at least one had not undergone any previous interaction. In the case of high-energy reactions between heavy ions¹ this led to some disagreements with the experiment. The

present work deals mainly with the effects of these "cascade-cascade" (CC) interactions on the predictions of the intranuclear cascade model.

Section II describes our method of treating the CC interactions. In Sec. III some proton and pion inclusive cross sections are compared with experimental results. Section IV deals with two-particle correlations. A number of systematic studies are discussed in Sec. V. Our conclusions are presented in Sec. VI.

II. THE CASCADE-CASCADE INTERACTIONS

The interaction of a single particle (proton, pion) with a nucleus via an intranuclear cascade involves a relatively small number of cascade particles. The evolving particle density outside the target Fermi sea in such an interaction is small, and the relative distances between the energetic particles are in general quite large. Thus the model neglected the scattering between any pair of cascade particles. In our earlier version of the intranuclear cascade model for nucleus-nucleus collisions¹ we made the same approximation, although this approximation is much less justified in this case. In the present paper we discuss the results of calculations in which CC interactions are included.

For the purpose of calculating interactions between the (discrete) cascade particles and the Fermi sea particles of the projectile or target the latter distributions are considered continuous. Thus the calculation of the interactions involves one discrete particle and one continuous density. We preferred to keep this method also for the calculation of the CC interactions. This was achieved by assuming a continuous cascade particle density. Each cascade particle is represented, in its rest frame, by a spherical Gaussian density distribution $\rho(r)$ centered at its discrete

position with a standard deviation of 1 fm. Each cascade particle may thus interact with the continuous Fermi sea distributions of the target and projectile and the continuous distribution of its fellow cascade particles. The only restriction is that two given cascade particles cannot interact more than once, until at least one of them interacted with a third particle. The procedure conserves energy and momentum but does not conserve angular momentum in each CC interaction.

III. PROTON AND PION INCLUSIVE SPECTRA

As in Ref. 1, our present calculation does not include complex particle production in the cascade process. We count the individual protons and neutrons leaving the system and disregard the fact that they may actually be constituents of d , t , α , etc. Therefore our proton spectra should be compared with the experimental "summed charge" spectra including both "free" protons and those bound in complex clusters.

In Figs. 1 and 2 summed charge spectra of Ref. 3 are compared with our new calculation. (In the following we use the "slow rearrangement" version of density depletion.¹⁾ Evaporation particles are not included in our calculation.

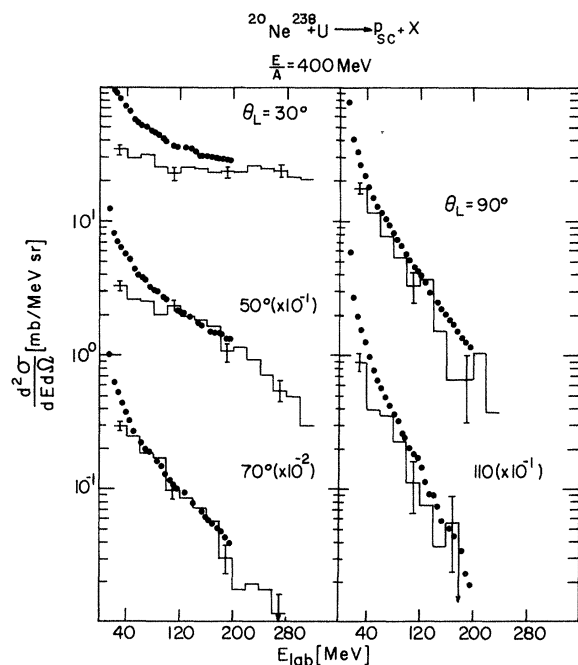


FIG. 1. The inclusive double-differential cross section for the emission of nucleon charges in the reaction $^{20}\text{Ne} + ^{238}\text{U}$ at a bombarding energy of $E/A = 400$ MeV. The dots represent the experimental results of Ref. 3. The histograms show the calculated results including the CC interactions.

For the two systems shown, $^{40}\text{Ne} + ^{238}\text{U}$ at $E/A = 400$ MeV and $^{40}\text{Ar} + ^{40}\text{Ca}$ at $E/A = 1.05$ GeV, the agreement with experiment is of similar quality to that of the proton inclusive spectra of Ref. 1. The comparison with the summed charge experimental spectrum reveals a serious underestimate of the low-energy part ($E < 80$ MeV) of the spectra. This discrepancy is larger for forward angles and is more pronounced in the heavier system. A part of this discrepancy (although probably not all of it) may be due to our neglect of the evaporation particles.

The lack of sensitivity of the inclusive proton cross sections to the CC rescattering may be understood in terms of following considerations: In peripheral collisions there is little CC rescattering due to the low density of the cascade particles. On the other hand, "central" collisions leading to a relatively high density of cascade particles undergo appreciable "thermalization" even without the CC rescattering, and therefore this rescattering has little effect on the outgoing spectrum.

The situation is quite different for the pion inclusive cross sections. In Fig. 3 the calculations including and excluding the CC scatterings are

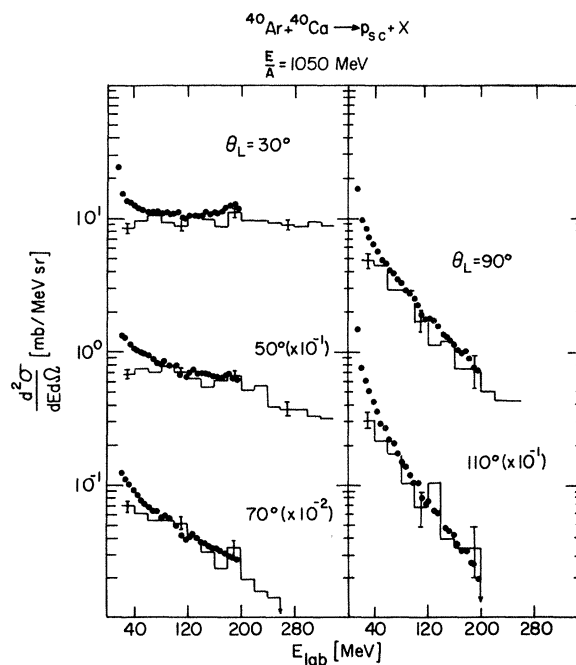


FIG. 2. The inclusive double-differential cross section for the emission of nucleon charges in the reaction $^{40}\text{Ar} + ^{40}\text{Ca}$ at a bombarding energy of $E/A = 1050$ MeV. The dots represent the experimental results of Ref. 3. The histograms show the calculated results including the CC interactions.

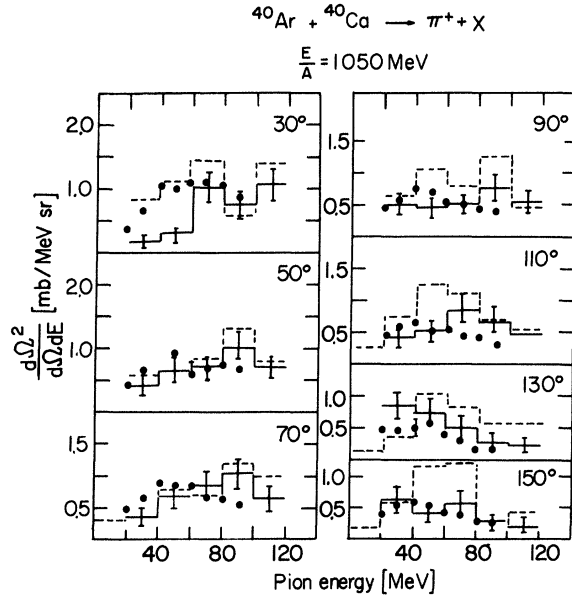


FIG. 3. The inclusive double-differential cross section for emission of π^+ in the reaction $^{40}\text{Ar} + ^{40}\text{Ca}$ at a bombarding energy of $E/A = 1050 \text{ MeV}$. The dots represent the experimental results of Ref. 4. The solid line histograms are the calculated results including the CC interactions, and the broken-line histograms are calculated results excluding the CC interactions.

compared with the experimental results.⁴ Here the CC rescatterings cause a reduction of the number of emitted pions. Although this leads to an underestimate of the low-energy forward-

angle part of the spectrum, there is a significant improvement for $\theta > 50^\circ$. The lower pion inclusive cross sections are probably the result of the increased pion capture probability via the $\Delta + N \rightarrow 2N$ reaction¹ due to the increased particle density seen by the Δ resonances as a result of the inclusion of the cascade particles in the calculation.

In Fig. 4 the calculated invariant cross section for π^+ emission in the $^{40}\text{Ar} + ^{40}\text{Ca}$ reaction at $E/A = 1.05 \text{ GeV}$ is shown on a P_\perp vs rapidity plot. In addition to forward-backward peaking, which is characteristic of $p+p$ reactions,⁴ there is some enhancement of the pion yield at the midrapidity, i.e., at the center of mass of the target-projectile system, and at a perpendicular momentum of about $0.7m_\pi$. Experimentally⁴ the invariant cross section shows a more pronounced peak at the mid-rapidity at a perpendicular momentum of $0.4m_\pi$. The effect has been interpreted⁵ in terms of collective hydrodynamic flow. It is therefore of interest to note that qualitatively the effect is also reproduced by the INC model. It should be noted that the present calculation neglects the deflection of the outgoing pions in the Coulombic field of the target, projectile, and the other emitted charged particles.

IV. TWO-PARTICLE CORRELATIONS

The measurement of two-particle correlations in high-energy heavy-ion collisions yield informa-

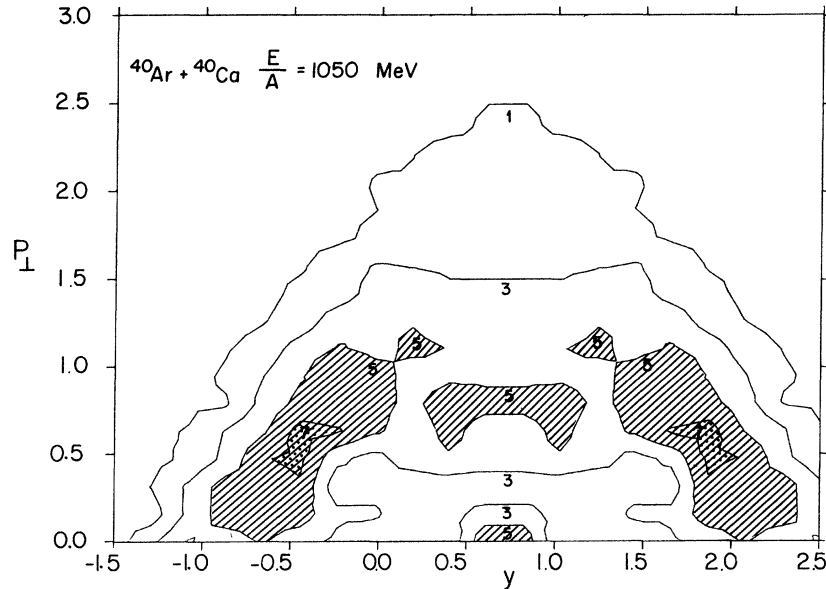


FIG. 4. Contours of constant Lorentz-invariant π^+ cross sections $d^2\sigma/pd\Omega dE$ in units of $b/(\text{sr GeV}^2/c)$ as a function of perpendicular pion momentum P_\perp in units of $m_\pi c$ and rapidity y , for the reaction $^{40}\text{Ar} + ^{40}\text{Ca}$ at a bombarding energy of $E/A = 1050 \text{ MeV}$. The target rapidity is $y_T = 0$, the projectile rapidity $y_P \approx 1.4$, and the center of mass rapidity is $y_{c.m.} \approx 0.7$. Areas of higher cross sections are shaded.

tion on the relative amount of single collision processes versus multiple collision processes. The intranuclear cascade model is well suited to deal correctly with such a mixture of processes. The information about the relative importance of the two components of the nucleus-nucleus reaction is of interest for evaluating the more simplistic models—the “fireball-firestreak” models^{6,7} which assume total thermalization (only multiple collision processes) and the “single knockout” model which assumes only single collisions.⁸

In Fig. 5 we compare the two-proton correlations calculated with CC scattering with the experimental results of Nagamiya *et al.*⁹ for $E/A = 800$ MeV $^{12}\text{C} + ^{12}\text{C}$, $^{40}\text{Ar} + ^{40}\text{Ar}$, and $^{40}\text{Ar} + ^{208}\text{Pb}$ reactions. Our definition of the two-particle correlation follows here that of Ref. 9: If in a given cascade a particle (“trigger particle”) is emitted in the laboratory polar angle $\theta_{\text{telescope}}$ (“telescope angle”), the particles in the polar angular range $35^\circ < \theta < 45^\circ$ (“tag counter angle”) are examined and their azimuthal angles with respect to the trigger particle determined. C is defined as the ratio of the number of such particles in the azimuthal range $\phi = 180^\circ \pm \Delta\phi$ ($\Delta\phi = 10^\circ$) to the average number of particles in the azimuthal ranges $\phi = \pm 90^\circ \pm \Delta\phi$. The azimuthal angle of the trigger particle is $\phi = 0$. C is large (>1) if the number of interactions per particle in the collision is small, whereas $C=1$ for a thermal distribution.

In the calculation presented in Fig. 5 the trigger particles are protons with energy $E_p > 100$ MeV and charged pions of any energy. For $^{12}\text{C} + ^{12}\text{C}$ both the experimental and calculated results show $C > 1$ and both peak at $\theta_{\text{telescope}} = 40^\circ$. The calculated maximum value of C is $C=1.7$, a little higher than the experimental one $C=1.5$. Still, within the statistical errors the agreement with experiment is satisfactory.

As expected, the introduction of the CC rescatterings has a significant effect on the two-particle correlations. Comparing our present $^{12}\text{C} + ^{12}\text{C}$ results with those of Ref. 1 (see Fig. 5) shows a large decrease of the C function. In the $^{12}\text{C} + ^{12}\text{C}$ reaction the CC collisions are only 26% of all collisions, yet they suffice to wash out a significant portion of the correlations.

The results for $^{40}\text{Ar} + ^{40}\text{Ar}$ agree very well with experiment. Both experiment and calculations show a slight positive correlation. For $^{40}\text{Ar} + ^{208}\text{Pb}$ the experimental results seem to give a somewhat negative C , indicating perhaps a slight shadowing.⁹ The calculated results are consistent with the value $C=1$ (no correlation). Comparison with Fig. 11 of Ref. 1 does not reveal an appreciable

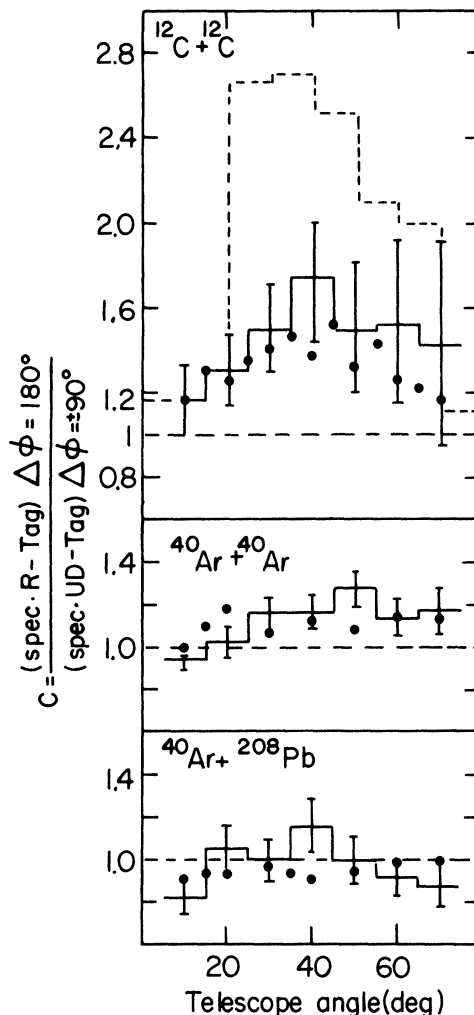


FIG. 5. The ratio C of “in plane” ($\Delta\phi = 180^\circ$) to “out of plane” ($\Delta\phi = \pm 90^\circ$) two-particle correlations as a function of the polar angle (telescope angle) of one of the particles. The second particle is detected at a polar angle of $40 \pm 5^\circ$. $\Delta\phi$ is the difference in azimuthal angle between the two particles. The figure shows the data for $^{12}\text{C} + ^{12}\text{C}$, $^{40}\text{Ar} + ^{40}\text{Ar}$ (exp. $^{40}\text{Ar} + \text{KCl}$), and $^{40}\text{Ar} + ^{208}\text{Pb}$ at a bombarding energy of $E/A = 800$ MeV. The dots represent the experimental results of Ref. 9. The solid-line histograms are the calculated results including the CC interactions and the broken-line histograms are the calculated results excluding the CC interactions.

effect of the CC rescatterings on the C function for $^{40}\text{Ar} + ^{40}\text{Ar}$ or $^{40}\text{Ar} + ^{208}\text{Pb}$ since C is already close to 1 even without the inclusion of CC rescattering.

V. SYSTEMATIC STUDIES

In Ref. 1 we have addressed ourselves to the question of the dependence of proton multiplicity on the impact parameter, and found that multi-

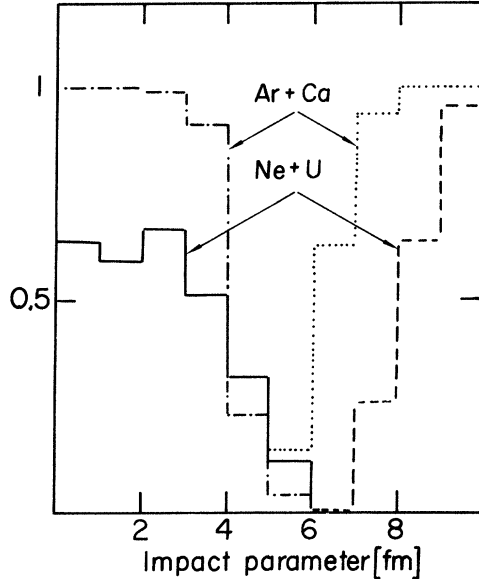


FIG. 6. The ratio of the multiplicity-selected proton inclusive cross section to the total proton inclusive cross section as a function of impact parameter. The solid line represents the $\sigma_{m \geq 20} / \sigma_{\text{tot}}$ ratio for $^{20}\text{Ne} + ^{238}\text{U}$ at $E/A = 400$ MeV and the dashed line represents the ratio $\sigma_{m \leq 5} / \sigma_{\text{tot}}$ for the same reaction. The dash-dotted line represents the ratio $\sigma_{m \geq 20} / \sigma_{\text{tot}}$ for $^{40}\text{Ar} + ^{40}\text{Ca}$ at $E/A = 1050$ MeV and the dotted line represents the ratio $\sigma_{m \leq 5} / \sigma_{\text{tot}}$ for the same reaction.

plicity selection is a reasonable procedure for selecting specific impact parameter intervals. Figure 6 shows this point when CC rescattering is included. For $^{20}\text{Ne} + ^{238}\text{U}$ at $E/A = 400$ MeV and $^{40}\text{Ar} + ^{40}\text{Ca}$ at $E/A = 1050$ MeV the probabilities of the occurrence of extremely high proton multiplicities ($m \geq 20$) and extremely low proton multiplicities ($m \geq 5$ for $^{20}\text{Ne} + ^{238}\text{U}$ and $m \geq 6$ for $^{40}\text{Ar} + ^{40}\text{Ca}$) are shown as a function of impact parameter. For both systems there is a clear separation of the impact parameters contributing to the two classes of multiplicities.

Figures 7 and 8 show the impact parameter distribution of events triggered by a proton of $E > 200$ MeV for different scattering angles of the trigger particle for two systems: $^{20}\text{Ne} + ^{238}\text{U}$ at $E/A = 400$ MeV and $^{40}\text{Ar} + ^{40}\text{Ca}$ at $E/A = 1050$ MeV. In the $^{20}\text{Ne} + ^{238}\text{U}$ case a slight preference for lower impact parameters by triggering with more backward protons is seen. No significant effect of this kind is seen in the $^{40}\text{Ar} + ^{40}\text{Ca}$ case. A similar analysis of $^{40}\text{Ar} + ^{40}\text{Ca}$ case, with a charged pion serving as a trigger (Fig. 8), shows a more pronounced preference for small impact parameters for events triggered with backward pions.

The question of the average number of interactions of a particle before it leaves the interaction region was already mentioned in the discussion

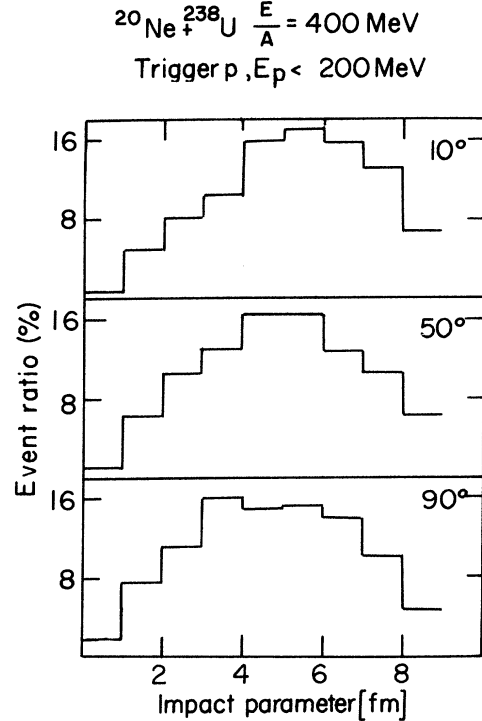


FIG. 7. The probability of events in which a proton of energy $E_p < 200$ MeV was emitted at $\theta = 10^\circ$ (upper graph), at $\theta = 50^\circ$ (middle graph), and at $\theta = 90^\circ$ (lower graph) as a function of the impact parameter. The reaction is $^{20}\text{Ne} + ^{238}\text{U}$ at $E/A = 400$ MeV.

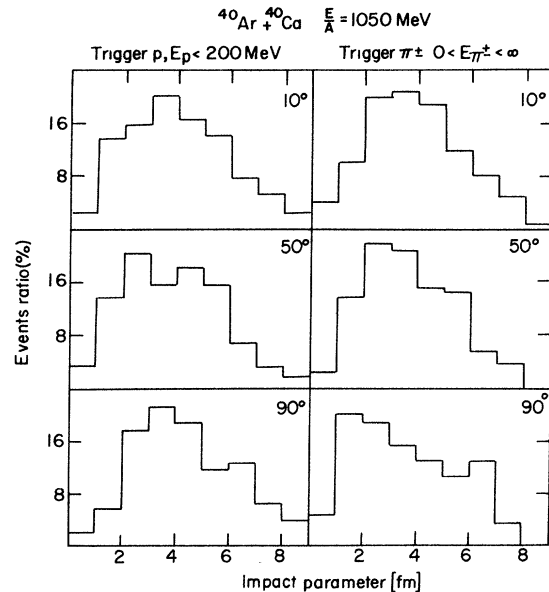


FIG. 8. The probability of events in which a trigger particle was emitted at $\theta = 10^\circ$ (upper row), at $\theta = 50^\circ$ (middle row), and at $\theta = 90^\circ$ (lower row) as a function of impact parameter. The reaction is $^{40}\text{Ar} + ^{40}\text{Ca}$ at $E/A = 1050$ MeV. The trigger particle is a proton of energy $E_p < 200$ MeV at the left column and a charged pion of any energy at the right column.

of the two-particle correlations. We stated in Ref. 1 that this is a somewhat ambiguous concept. There is no simple way to generalize the definition used in Ref. 1 to be useful in the present calculation which includes cascade-cascade rescattering. Still, the proportion of "first generation" particles among all the particles leaving the system is a well-defined number. We define by first generation particles only pairs of particles for which *both* partners underwent only a single elastic collision which lifted them out of their respective Fermi seas. Neglecting Fermi motion these particles obey strictly the two-body kinematics of a nucleon of projectile velocity with a stationary nucleon, and they are responsible for the bulk of two-particle correlations discussed in Sec. IV.

Figure 9 shows the percentage of first generation protons and neutrons in the inclusive nucleon

spectrum as a function of impact parameter for the $^{12}\text{C} + ^{12}\text{C}$ system at two energies, $E/A = 400$ and 800 MeV. Even for this light system the proportion of the first generation particles is quite small at $E/A = 800$ MeV; only 20% of pure two-body scattering even at very large impact parameters. For central collisions of partly overlapping nuclei (the hard sphere radius of ^{12}C is 2.15 fm) we have less than 10% of first generation particles. This result was also indicated by the lowering of two-particle correlations with the addition of the cascade-cascade rescattering. (Our energy cutoff causes a small reduction of the first generation particles. In a collision between a very energetic and an almost stationary particle there is a large probability of small momentum transfer. Thus one of the outgoing particles may fall below our energy cutoff and both partners are then removed from the first

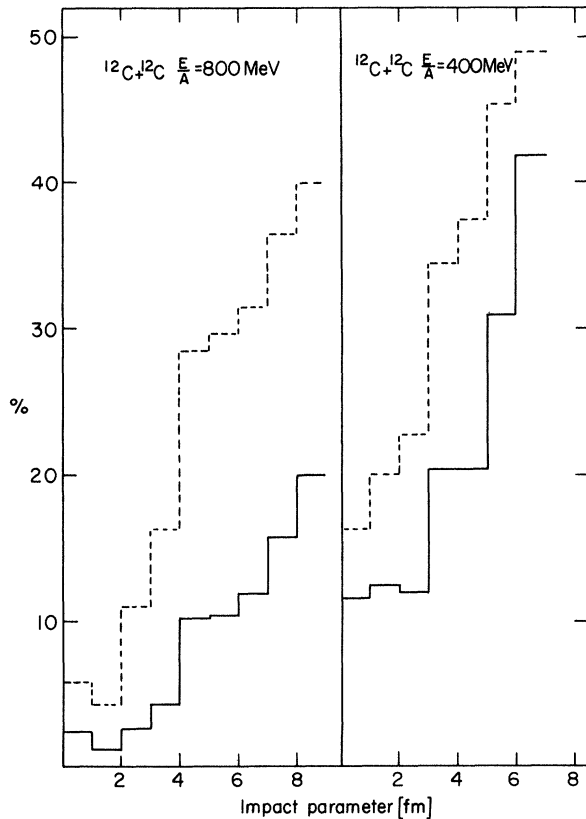


FIG. 9. Percentage of the first generation (see text) nucleons as a function of impact parameter for the reactions $^{12}\text{C} + ^{12}\text{C}$ at $E/A = 400$ MeV and $E/A = 800$ MeV. The solid lines denote the average values (1st moment) and the broken lines denote the standard deviation (2nd moment).

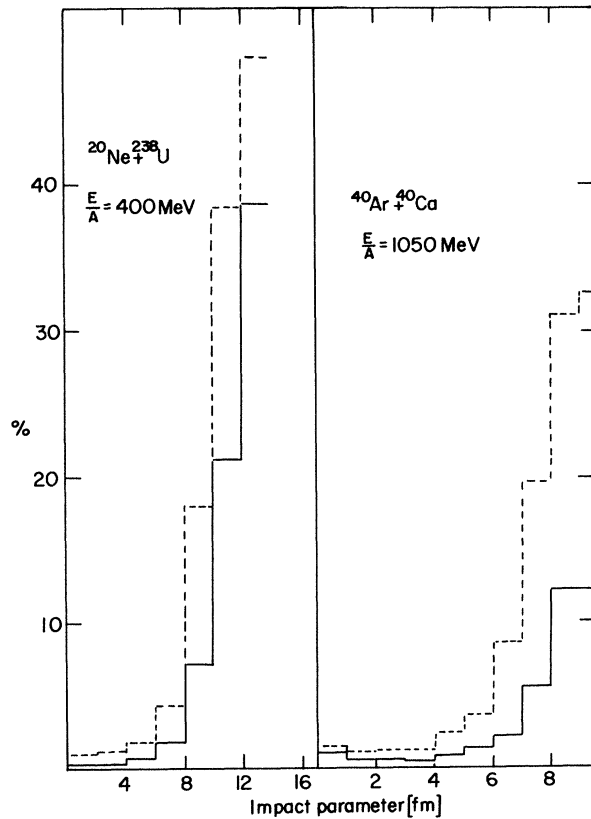


FIG. 10. Percentage of the first generation (see text) nucleons as a function of impact parameter for the reactions $^{20}\text{Ne} + ^{238}\text{U}$ at $E/A = 400$ MeV and $^{40}\text{Ar} + ^{40}\text{Ca}$ at $E/A = 1050$ MeV. The solid lines denote the average values (1st moment) and the broken lines denote the standard deviation (2nd moment).

generation spectrum.) The isobar production also has a quenching effect on the pure two-body-kinematics component of the spectrum. This can be clearly seen by comparing the results for $^{12}\text{C} + ^{12}\text{C}$ at $E/A = 800$ and 400 MeV. We notice a large decrease in the percentage of first generation nucleons at the higher energy due to the higher probability of isobar production in the first collision.

Figure 10 shows the percentage of first generation nucleons in the nucleon inclusive spectrum as a function of impact parameter for $^{20}\text{Ne} + ^{238}\text{U}$ at $E/A = 400$ MeV and $^{40}\text{Ar} + ^{40}\text{Ca}$ at $E/A = 1.05$ GeV. The low proportion in the $^{40}\text{Ar} + ^{40}\text{Ca}$ case can again be attributed to the enhanced probability of isobar production in the first interaction.

Integrating over impact parameter leads to a fraction of first generation nucleons of 16.8% for $^{12}\text{C} + ^{12}\text{C}$ at $E/A = 400$ MeV, 4.5% for $^{12}\text{C} + ^{12}\text{C}$ at $E/A = 800$ MeV, 1.4% for $^{40}\text{Ar} + ^{40}\text{Ca}$ at $E/A = 1.05$ GeV, and 2.2% for $^{20}\text{Ne} + ^{238}\text{U}$ at $E/A = 400$ MeV.

VI. SUMMARY

The inclusion of CC rescattering in the INC model generally improves the agreement with experimental results. Whereas the proton inclusive cross sections are rather insensitive to the CC rescattering, the pion inclusive cross section is generally reduced, improving the agreement with experiment at backward angles. The two-particle correlations calculated with CC rescatterings agree well with experiment even for the light $^{12}\text{C} + ^{12}\text{C}$ system. The calculations show that the choice of the trigger-particle (i.e., telescope) angle does not affect the impact parameter distribution of the collisions if the trigger particle is a proton, and does affect it only slightly if the trigger particle is a pion. The investigation of the number of nucleons undergoing only a single collision before leaving the interaction region indicates that multiple scattering effects are important in both central and peripheral interactions.

¹Y. Yariv and Z. Fraenkel, *Phys. Rev. C* **20**, 2227 (1979).

²K. Chen, Z. Fraenkel, G. Friedlander, J. R. Grover, J. M. Miller, and Y. Shimamoto, *Phys. Rev.* **166**, 949 (1969).

³S. Sandoval, H. H. Gutbrod, W. G. Meyer, A. M. Poskanzer, R. Stock, G. Gosset, J.-C. Jourdain, C. H. King, G. King, Ch. Lukner, Nguyen Van Sen, G. D. Westfall, and K. L. Wolf, *Phys. Rev. C* **21**, 1321 (1980).

⁴K. Wolf, H. H. Gutbrod, W. G. Meyer, A. M. Poskanzer, A. Sandoval, R. Stock, J. Gosset, C. H. King, G. King, Nguyen Van Sen, and G. D. Westfall, *Phys.*

Rev. Lett. **42**, 1448 (1979).

⁵W. Scheid, B. Muller and W. Greiner, *Phys. Rev. Lett.* **32**, 741 (1974).

⁶G. D. Westfall, J. Gosset, P. J. Johansen, A. M. Poskanzer, W. G. Meyer, H. H. Gutbrod, A. Sandoval, and R. Stock, *Phys. Rev. Lett.* **37**, 1202 (1976).

⁷W. D. Myers, *Nucl. Phys.* **A296**, 177 (1978).

⁸R. L. Hatch and S. E. Koonin, *Phys. Lett.* **81B**, 1 (1979).

⁹S. Nagamiya, L. Anderson, W. Bruckner, O. Chamberlain, M.-C. Lemaire, S. Schnetzer, G. Shapiro, H. Steiner, and I. Tanihata, *Phys. Lett.* **81B**, 147 (1979).